NDT&E International 70 (2015) 9–15

Contents lists available at ScienceDirect

NDT&E International

journal homepage: www.elsevier.com/locate/ndteint

# Nonlinear ultrasonic evaluation of the fatigue damage of adhesive joints

Guoshuang Shui [a,*], Yue-sheng Wang [a,*], Peng Huang [a], Jianmin Qu [b]

[a] Department of Mechanics, Beijing Jiaotong University, Beijing 100044, China
[b] Department of Civil and Environmental Engineering, Northwestern University, Evanston, IL 60208-3109, USA

ARTICLE INFO

*Article history:*
Received 24 April 2014
Received in revised form
12 November 2014
Accepted 17 November 2014
Available online 18 December 2014

*Keywords:*
Nonlinear ultrasonics
Fatigue damage
Adhesive joints
Non-destructive evaluation

ABSTRACT

An experimental method based on the nonlinear ultrasonic technique is presented to evaluate fatigue damage of an adhesive joint. In this paper, specimens made from AZ31 magnesium–aluminum alloy bonded through an epoxy layer are subjected to a fatigue load. The ultrasonic harmonics generated due to damage within the adhesive layer are measured; and the acoustic nonlinearity parameter (ANP) based on the fundamental and second harmonics is determined. The results show that the normalized ANP increases with the fatigue cycles. Furthermore, a theoretical model with different interfacial compression and tension stiffness is proposed to interpret the generation of second harmonics.



## 1. Introduction

Adhesive joints are widely used in various industrial applications, such as safety-critical structures in the aerospace and automotive industries. Adhesively bonded structural components usually provide many advantages over conventional mechanical fasteners. Among these advantages are lower structural weight, lower fabrication cost, and improved damage tolerance [1,2]. For example, advances in aerospace technology have been made possible through the use of lightweight materials and weight-saving structural designs. Joints, in particular, have been and continue to be areas in which weight can be trimmed from an airframe through the use of novel attachment techniques.

With the increasing use of adhesive bonded structures, corresponding methods for evaluation and testing of the structural integrity and quality of bonded joints have been widely investigated and developed for the purpose of structural health monitoring [3–5]. Non-destructive characterization for quality control and remaining life prediction has been a key enabling technology for the effective use of adhesive joints. Conventional linear ultrasonic techniques can detect flaws such as delamination, cracks, and voids in the adhesive joints. However, more important to the bond quality is the adhesive strength. Although in principle, strength cannot be measured non-destructively, the slight nonlinearity in the material may indicate material degradation or the onset of failure [6]. Furthermore, microstructural variations due to aging may also cause change in the third order elastic constants, which are related to the acoustic nonlinear parameter (ANP) of the polymer adhesive.

It has been observed that higher harmonics of the fundamental frequency are generated when a harmonic ultrasonic wave propagates through a nonlinear material [7]. It is proposed that the material degradation creates nonlinearity which can be detected in the wave propagation characteristics [8,9]. Several theories have been developed to model this nonlinear effect. For example, Achenbach and Parikh [10] presented their theoretical investigation to obtain information on the adhesive bond strength from ultrasonic test results. Using the postulate that failure of the adhesive bond is preceded by nonlinear behavior at the interface, they obtained a nonlinear parameter that correlates to joint strength. Based on a microscopic description of the nonlinear interface binding force, a quantitative method was presented by Pangraz and Arnold [11]. Tang et al. [12] measured the onset of nonlinearity in adhesive bonds by subjecting to static loads simultaneously with the ultrasonic testing. The degradation of the adhesive bond was induced by cyclic fatigue loading. The deterioration due to cyclic fatigue is identified by the reduction of the linear portion of the stress–strain curve without any change in slope in the linear range. Furthermore, Delsanto et al. [13,14] developed a spring model to simulate the ultrasonic wave propagation in non-classical (hysteretic) nonlinear media. Vanaverbeke et al. [15] proposed a multiscale model for the two-dimensional (2D) nonlinear wave propagation in a locally microdamaged medium, and presented numerical simulations in view of nondestructive testing applications. An et al. [16] developed a rigorous nonlinear spring model under the normal incidence of both longitudinal and SH waves. The numerical simulations show the accuracy and applicability of their model for a

* Corresponding authors.
*E-mail addresses:* gsshui@bjtu.edu.cn (G. Shui), yswang@bjtu.edu.cn (Y.-s. Wang).

http://dx.doi.org/10.1016/j.ndteint.2014.11.002
0963-8695/

thin layer between two solids under the condition of small ratio of thickness to wavelength.

In the meanwhile, ultrasonic guided waves have been used to analyze adhesive or diffusion bonded joints. For example, Nagy and Adler [17] studied guided waves in adhesive layers between two half-spaces, demonstrating that the resulting dispersion curves are relatively insensitive to the properties of the adhesive layer. Rohklin and Wang [18] examined Lamb waves in lap–shear joints, including the development of an analytical spring model. Rose et al. [19] developed dispersion curves for titanium diffusion bonds and examined frequency shifts and spectral peak-to-peak ratios of different bonded states. Lowe and Cawley [20] analyzed the sensitivity of adhesive bond properties on guided waves using a three-layered model. Heller et al. [21] combined laser ultrasonic techniques with the 2D fast Fourier transform (FFT) to characterize adhesive bond properties. Seifried et al. [22] used analytical and computational models to develop a quantitative understanding of the propagation of guided Lamb waves in multi-layered, adhesive bonded components.

In this paper, the ANP is used to characterize the degradation of an adhesive joint made from epoxy resin between two aluminum plates. Ultrasonic through-transmission tests were conducted on samples cured under various conditions. The magnitude of the second order harmonic was measured and the corresponding ANP was evaluated. These experimentally measured ANPs, as functions of degradation, are then used to quantitatively characterize the condition of the adhesive bond. A fairly good correlation between the fatigue cycle and the ANP is observed. Furthermore, the experimentally observed second harmonic generation is interpreted by developing an analytical model. The results show that the ANP can be used as a good indicator of the adhesive strength for adhesive joints.

## 2. Experimental procedure

As shown in Fig. 1, the test sample is an overlap joint of two aluminum plates bonded together by an adhesive layer. The adhesive is a kind of bisphenol epoxy resin with epoxy value of 0.441 mol/100 g. The aluminum plate is made of AZ31 magnesium–aluminum alloy, with the yielding stress 199 MPa, elastic modulus 46 GPa, Poisson's ratio 0.27 and density 1770 kg/m$^3$. As illustrated in Fig. 1, the bonded area of the specimen is 30 mm × 24 mm. The adhesive (bondline) thickness is generally less than 1 mm and the adherend's thickness is about 6.5 mm. The aluminum plates were anodized and primed prior to application of the adhesive. The joints were then put into a temperature/pressure oven for curing. They were firstly cured for two hours with a temperature of 80 °C, and then cured for another two hours with a temperature of 160 °C. All samples used in this study were prepared under the same conditions.

A schematic diagram for the experimental setup is shown in Fig. 2. The transmitting transducer was driven by a tone burst signal of 6 cycles at 5 MHz. The receiving transducer was used to detect the fundamental and second harmonics of longitudinal ultrasonic waves passing through the adhesive joint. The central frequencies of transmitting and receiving transducers are, respectively, 5 MHz and 10 MHz. The tone burst signal was generated by Ritec SNAP-0.25-7-G2 nonlinear measurement system with the high-power gated amplifier. Before driving the transmitting transducer, the high voltage signal passed through a 50 Ω termination, an attenuator and a set of low-pass filter so that the transient behavior and high frequency component from the amplifier were suppressed. This nonlinear measurement system can provide a more monochromatic ultrasonic sine wave signal with higher quality, and this will decrease the acoustic nonlinearity from the signal considerably.

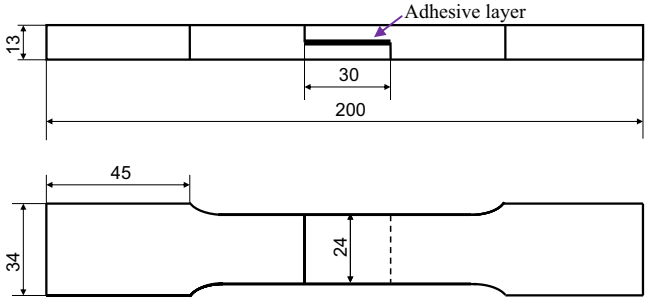


**Fig. 1.** Dimension of two aluminum plates bonded through an adhesive layer (unit: mm). (For interpretation of the references to color in this figure legend, the reader is referred to the web version of this article.)

Although the multi-reflection can take place between the upper/lower surface and interface in the experimental samples, the reflected waves reach the Receiver about 0.6 μs later than the last cycle of the waves passing through the adhesive joint reach the Receiver. So there is no multi-reflective influence in the received signal. A typical longitudinal wave signal acquired is shown in Fig. 3. (One should notice that 9.0 μs shown in this figure, which is owing to the setting of the oscilloscope, is NOT the flight time of the wave.) The sampling rate of the oscilloscope is 1.25 GS/s. The signal of an entire length consists of a transient part at the beginning, a steady state portion, and finally the turnoff ringing at the end. To make sure that only the steady-state part of the tone burst signal was used, a Hanning window was applied to the acquired time-domain signal for Fast Fourier Transform (FFT). Therefore, only the data points within the steady-state part were selected and then transformed to the frequency domain where the amplitudes of the fundamental and higher order harmonics of the detected waves become visible. Fig. 4 shows the amplitudes of the fundamental ($A_1$) and second ($A_2$) harmonics in the frequency domain, respectively.

## 3. Experimental results

During the experimental measurements, ten samples were selected to be fatigued. The fatigue loading is parallel to the adhesive layer, as shown in Fig. 2. The maximum load for five of the samples was 2.5 kN; and the maximum load for another five was 3.0 kN. The fatigue tests were interrupted to perform the nonlinear ultrasonic measurements at different numbers of fatigue cycles.

Following Refs. [23,24], the ANP of the adhesive is defined by

$$\beta = \frac{8A_2}{A_1^2 hk^2} \tag{1}$$

where $A_1$ is the amplitude of the fundamental harmonic wave; $A_2$ is the amplitude of the second harmonic wave; $h$ is the propagation distance; and $k$ is the wave number. For longitudinal waves with a fixed frequency and a fixed transmitting distance, the ANP, $\beta$, is only proportional to $A_2/A_1^2$. Therefore, in this measurement, we use, for convenience, a relative ANP defined as

$$\beta' = \frac{A_2}{A_1^2} \tag{2}$$

Because there will be some level of variability associated with the initial microstructure of each specimen, the measured ANPs will be normalized by the value ($\beta'_0$) measured in each undamaged specimen before any mechanical load is applied. This normalization procedure removes some of the variability associated with the initial microstructures of each specimen, enables a direct comparison of the acoustic nonlinearity evolution of all the specimens tested, and normalizes the nonlinearity associated with the transmitting piezoelectric transducers. The evolution of the normalized ANP, $\beta'/\beta'_0$, as a function of the normalized fatigue life is shown in Fig. 5(a) for specimens 1–5 with the maximum load of 2.5 kN. Here, the fatigue

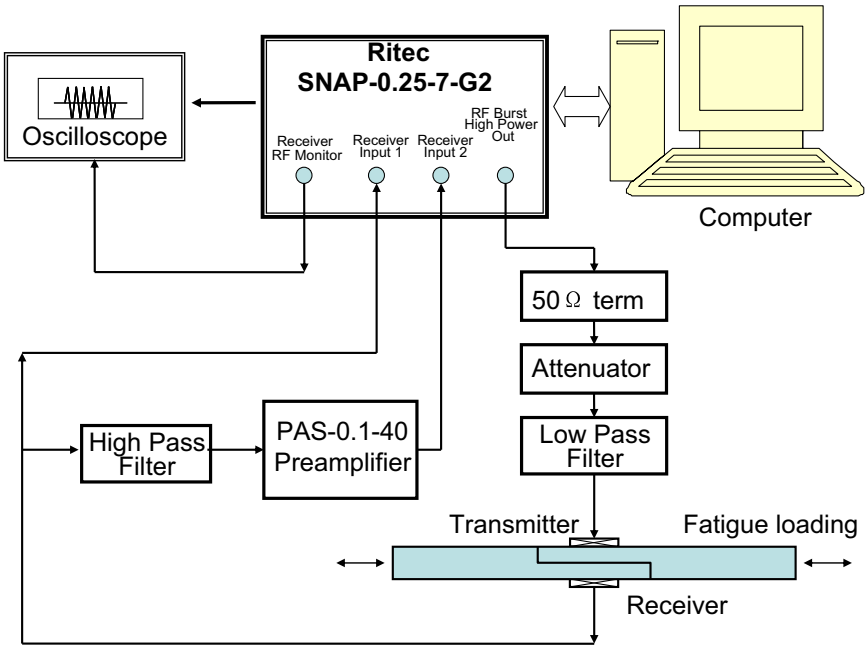


**Fig. 2.** Experimental setup for nonlinear measurement of an adhesive joint.

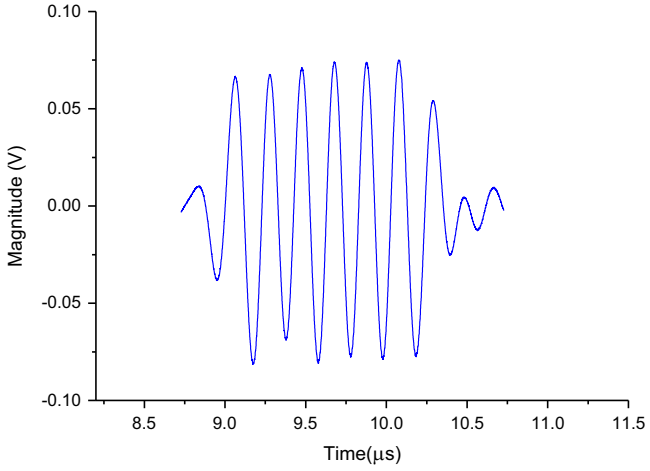


**Fig. 3.** Received nonlinear ultrasonic waves.

life means the fatigue cycle normalized to the total cycles of the whole specimen's life. The specimens 1–5 failed at 80, 91, 560, 281 and 97 cycles, respectively. Shown in Fig. 5(b) is the evolution of the normalized ANP as a function of the normalized fatigue life for specimens 6–10 with the maximum load of 3.0 kN. For this group, the specimens 6–10 failed at 111, 91, 310, 102 and 280 cycles, respectively.

It is shown in Fig. 5 that the normalized ANP increases with the fatigue life for both situations. Particularly, we can see that the rate of increase appears to be greater in the early stages, which implies that these nonlinear ultrasonic measurements can be used to quantitatively characterize the early damage of the adhesive joints. The measured data for different specimens show increasing scatter with increasing fatigue cycles, which is most likely due to uncertainties in material properties and cure of the adhesion. In fact, there is an inherent randomness in the evolution of fatigue damage during testing, which should manifest itself as a corresponding randomness in the resulting acoustic nonlinearity. For measurement procedure in the later stage of fatigue, the deformation associated with the increased fatigue cycle makes it difficult to consistently conduct the nonlinear measurement. But fortunately, our data explicitly show the dependence of the ANP on the fatigue cycles. Comparison of Fig. 5(a) and (b) shows that the maximum load has a little influence on the magnitude of the normalized ANP.

## 4. Theoretical model and discussion

In order to interpret the generation of higher harmonics, we present a nonlinear model of the adhesive layer in this section.

The ultrasonic wave propagation through the adhesive joint in the above measurements may be illustrated in Fig. 6. Two identical semi-infinite linear elastic solids (adherends 1 and 2) are joined together by a thin adhesive layer with thickness $h$. Lamé constant, shear modulus and mass density of the adherends are $\lambda$, $\mu$ and $\rho$, respectively; and those for the adhesive layer are $\overline{\lambda}$, $\overline{\mu}$ and $\overline{\rho}$, respectively. For an incident harmonic longitudinal wave with frequency $\omega$ propagating perpendicular to the adhesive layer, it will be reflected by the adhesive layer as well as transmitted through the adhesive layer. We denote the incident, reflected and transmitted waves as $P_0$, $P_1$ and $P_3$, respectively, and those in the adhesive layer as $P_2$ and $P_4$.

Maeva et al. [1] indicated that there are expected to be two possible sources of nonlinearity in an adhesively bonded structure. The first source is the adhesive material itself. The second source might be structural nonlinearities in the adhesive bond line, including weak bonds or zero volume (closed) disbonds. After some experimentation, it becomes apparent that the material nonlinearity has little relevance to a great many adhesion problems; it is an indication of the state of the material itself other than an indicator of the bond strength [1]. The structural nonlinearity is, however, often thought of as being directly linked to the strength or weakness of the bond itself. The extreme example of this is the case of an unbonded, clapping interface, which has been studied theoretically and experimentally for some time [1].

Structural nonlinearities in adhesively bonded joints may arise in a number of ways. Common to all of these is the location of the structural defect, typically in the very thin layer of adhesive bonding [1]. During in-service conditions adhesive joints can suffer from a number of defects due to loading, environmental attack or other

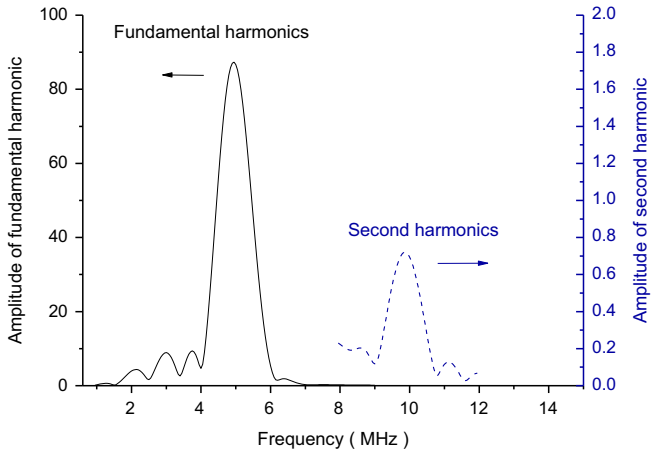


**Fig. 4.** Amplitudes of the fundamental and second harmonics of the ultrasonic waves.

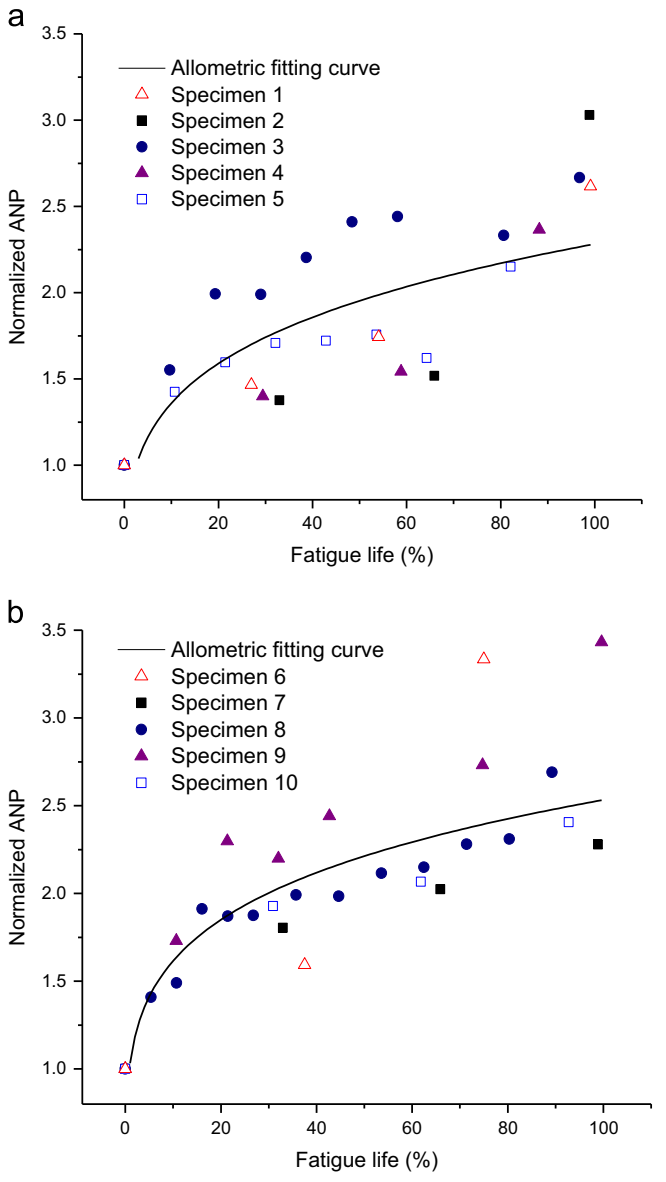


**Fig. 5.** Normalized ANP as a function of the percentage of fatigue life with the maximum load of 2.5 kN (a) and 3.0 kN (b).

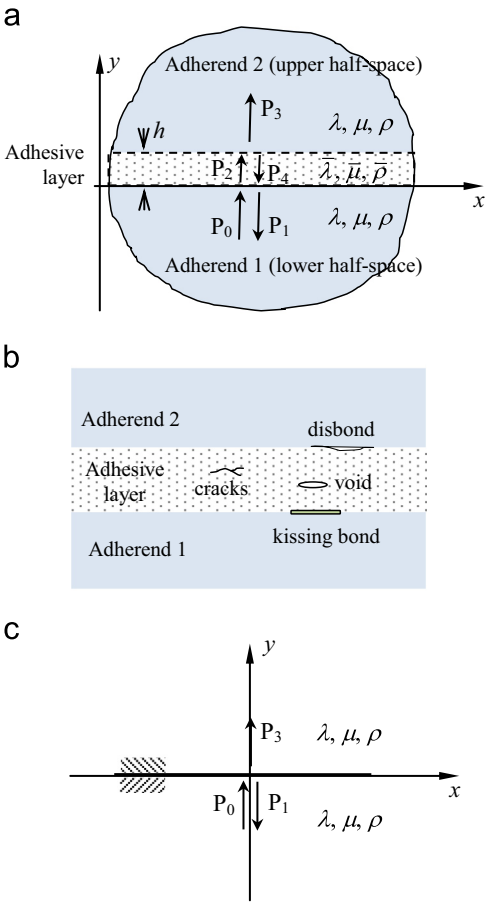


**Fig. 6.** Wave propagation in two adherends joined by an adhesive layer (a), typical defects in an adhesive layer appearing during in-service conditions [25] (b), and illustration of the theoretical nonlinear model (c).

reasons. These defects may include voids, cracks, disbond, kissing bond etc. as illustrated in Fig. 6(b) [25]. The overall strength of the joint depends on the behaviors of these defects under loading. Obviously, the tensile and compressional behaviors of the joint will be different. For instance, in the crack, disbond or kissing bond region, a potential mechanism for nonlinearity is the opening and closing of the contact as the wave passes; the so called “clapping” or “slapping” mechanism, or more generally, contact acoustic nonlinearity [26]. For perfectly flat surfaces in contact this results in a bi-linear stiffness response (with zero or low stiffness in the tensile region and high stiffness in the compressive region). More realistically, for rough surfaces in contact, there would be a more gradual shift from a low-stiffness, low-load region to a high-stiffness, high-load region [26]. If a purely sine harmonic ultrasonic wave is incident on a defected adhesive layer with such a stiffness nonlinearity the reflected and transmitted waves will contain a response including high harmonics; and the degree of harmonic generation provides information about the extent to which the defect behaves nonlinearly [26].

Based on the above analysis of which the details can be found in Refs. [1,26], we propose a nonlinear model by assuming that the damage of the adhesive layer will decrease its tension modulus while keeping its compression modulus unchanged during in-service. That is, the tension and compression moduli of the adhesive layer will be different. For simplicity in mathematics, the adhesive layer of finite thickness is replaced by a massless interface with zero thickness, as shown in Fig. 6(b). Consequently, the interface is modeled as a continuous array of springs with different tension and compression stiffness. At the interface, the boundary

condition can be written as

$$\begin{cases} \sigma_y(x) = K^+ \Delta u_y(x), \sigma_y, & \Delta u_y \geq 0 \\ \sigma_y(x) = K^- \Delta u_y(x), \sigma_y, & \Delta u_y \leq 0 \end{cases}, \tag{3}$$

where $\sigma_y(x)$ is the normal stresses at the interface; $\Delta u_y(x)$ is the displacement discontinuity at the interface; and $K^+$ and $K^-$ are stiffness of the interface in tension and compression, respectively.

When the ultrasonic wave propagates through the interface, the system will behave nonlinearly because of the different tension and compression stiffness. As shown in Fig. 6(c), for an incident harmonic longitudinal ultrasonic wave $P_0$ propagating in the $y$-direction with frequency $\omega$ and amplitude $A^{(0)}$, it can be written as

$$u_y^{(0)} = \mathrm{Re}\left\{A^{(0)} e^{i\zeta}\right\}, \tag{4}$$

where $\zeta = ky - \omega t$ with the wave number $k = \omega/c$ and $c$ being the longitudinal wave velocity in the adherend. When this harmonic ultrasonic wave is incident on the above bilinear interface, the reflected and transmitted waves will contain a response at the drive frequency as well as the higher harmonics due to nonlinearity. Therefore the transmitted wave $P_3$ can be written as:

$$u_y^{(3)} = \mathrm{Re}\left\{\sum_{m=0}^{\infty} A_m^{(3)} e^{im\zeta}\right\} \tag{5}$$

Similar to the experimental way, we defined a relative ANP $\beta_t'$ based on the amplitude of the fundamental harmonic wave $A_1^{(3)}$ and that of the second harmonic wave $A_2^{(3)}$ for the transmitted wave $P_3$, that is

$$\beta_t' = \frac{A_2^{(3)}}{\left[A_1^{(3)}\right]^2} \tag{6}$$

The solution of $\beta_t'$ is presented in Appendix A. Here, we consider the specimen used in our experiment, i.e. two adherends of AZ31 bonded through an epoxy layer. The relative ANP,$\beta_t'$, varying with $K^-/K^+$ is shown in Fig. 7. When $K^-/K^+ = 1$, the ANP is zero, which means that there is no interfacial damage in this situation. When damage appears within the adhesive layer, the tensile stiffness $K^+$ of the interface will decrease, leading to the increase of $K^-/K^+$ and thus the increase of the ANP. Therefore we can conclude that the ANP can be used to characterize the change of interface tensile stiffness or the degradation of the adhesive layer indirectly.

In damage mechanics, the damage variable $D$ is used to represent the development of microstructural damage in a continuum sense. This variable can be derived from the reduction of the elastic modulus simply as $D = 1 - \overline{E}/\overline{E}_0$, where $\overline{E}_0$ is the elastic modulus without damage. For the present problem, the damage variable $D$ can be expressed by using the tension stiffness $K^+$ and compression stiffness $K^-$ as $D = 1 - K^+/K^-$. Finally we can get the relation between the damage variable $D$ and the relative ANP $\beta_t'$ as shown in Fig. 8. We can see that the damage variable increases with the relative ANP increasing.

Many researches have been reported about the relation between material damage variable $D$ and fatigue cycles [27–29]. A simple empirical formulas was proposed in [29],

$$D = 1 - \left[1 - \left(\frac{N}{N_f}\right)^c\right]^m, \tag{7}$$

where $c$ and $m$ are parameters to be determined in an experimental way; $N$ and $N_f$ are fatigue cycles and fatigue life, respectively.

This equation will be applied in this paper to interpret the experimental results of the relation between the ANP and fatigue cycle. We found in our experiment that the ANP does not vanish before the specimen is loaded, i.e. $\beta' \neq 0$ when $N = 0$. This implies that initial damage does exist and should be considered in establishing the relation between the damage variable $D$ and relative fatigue cycles $N/N_f$. Therefore, we modify Eq. (5) as

$$D = 1 - (1 - D_0)\left[1 - \left(\frac{N}{N_f}\right)^c\right]^m \tag{8}$$

where $D_0$ is the initial damage variable regarding to the whole adhesive structure when $N = 0$. We can see that Eq. (6) satisfies two necessary conditions: $D = D_0$ when $N = 0$ and $D = 1$ when $N = N_f$. Considering Eq. (6) and the data in Fig. 8, we can get the relation between the normalized ANP $\beta_t'/\beta_{t0}'$ and relative fatigue cycles $N/N_f$. For example, if we take $D_0 = 0.1$, $m = 0.25$ and $c = 0.003$, we can get the relation between the normalized ANP and relative fatigue cycles based on the theoretical model. Fig. 9 shows the experiment measurement results with the maximum load of 3.0 kN (see Fig. 5b) and the data based on the theoretical model. It is seen that the ANP based on the theoretical model increases consistently with the measured results. We can come to the conclusion that different stiffness of the interface in tension and compression, caused by the damage in the adhesive layer, is one of the sources for the nonlinearity of ultrasonic waves transmitting through the adhesive structure. This provides us a

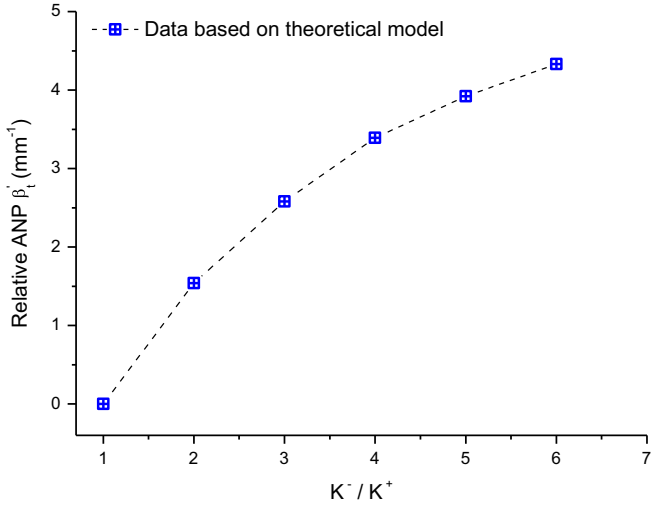


**Fig. 7.** Theoretical ANP as a function of the ratio of compression stiffness to tensile stiffness.

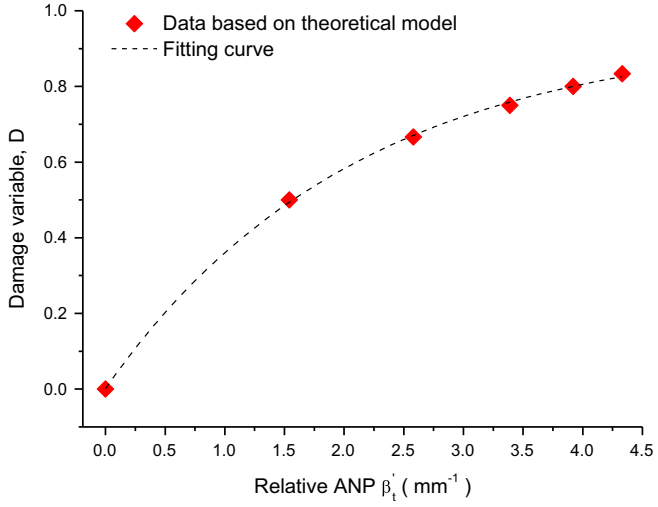


**Fig. 8.** Damage variable as a function of relative nonlinearity parameter.

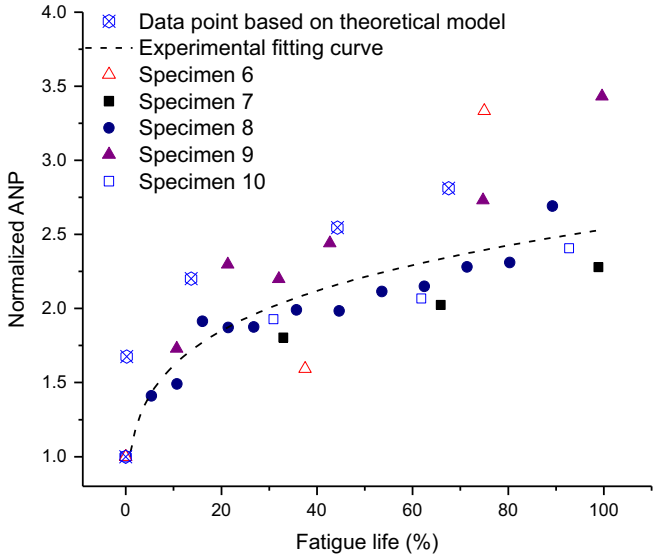


**Fig. 9.** Normalized ANP based on theoretical model and experimental measurement as a function of relative fatigue cycles.

possible way to detect the appearance and monitor the development of the defects in adhesive layers in engineering applications.

## 5. Conclusion

An experimental method based on the nonlinear ultrasonic technique is presented to evaluate fatigue damage of an adhesive joint. In this approach, specimens made from AZ31 magnesium–aluminum alloy bonded through an epoxy layer are subjected to a fatigue load. The ultrasonic harmonics generated due to damage within the adhesive layer are measured; and the acoustic nonlinearity parameter (ANP) based on the fundamental and second harmonics is determined. The results show that the normalized ANP increases with the fatigue cycles. Particularly, the rate of increase appears to be greater in the early stages. This demonstrates that the nonlinear ultrasonic measurement can be used to quantitatively characterize the early damage of adhesive joints. A theoretical model with different interfacial tension and compression stiffness is developed to interpret the generation of second harmonics. It is shown that the ANP based on the theoretical model increases consistently with the experimentally measured values although the empirical formulas relating the damage variable to the fatigue cycles proposed in the literature is employed. The present research, we believe, is relevant to practical structural health monitoring and life prediction for adhesive joints, and is expected to provide a promising way for the characterization and monitoring of degradation of adhesively layer effectively in both experimental and theoretical ways.

Finally we mention that the present theoretical model is still an approximation. There are many effects, e.g. the thickness, the mass, the material nonlinearity and the attenuation of the adhesive layer, that are excluded. A more precise model including these effects should be developed in our future work.

## Acknowledgments

Support by the National Natural Science Foundation of China (Grant no. 11472039) is greatly appreciated. The second author is also grateful to the support of National Basic Research Program of China (2010CB732104).

## Appendix A. Solution of the acoustic nonlinear parameter based on the bilinear interface model

We solve the nonlinear boundary value problem as illustrated in Fig. 6(c) where the interface follows the bilinear relation of Eq. (3). Based on Eqs. (4) and (5), the stress for the incident, reflected and transmitted waves can be written as

$$\sigma_y^{(0)} = \mathrm{Re}\left[ik(\lambda+2\mu)A^{(0)}e^{i\eta}\right],$$
$$\sigma_y^{(1)} = -\mathrm{Re}\left[ik(\lambda+2\mu)\sum_{m=1}^{\infty} mA_m^{(1)}e^{im\eta}\right],$$
$$\sigma_y^{(3)} = \mathrm{Re}\left[ik(\lambda+2\mu)\sum_{m=1}^{\infty} mA_m^{(3)}e^{im\eta}\right], \tag{A.1}$$

where $\eta=-\omega t$. Then the stress at the interface can be written as:

$$\begin{aligned}\sigma_y(\eta) &= \sigma_y^{(0)}(\eta,0)+\sigma_y^{(1)}(\eta,0)=\sigma_y^{(3)}(\eta,0)\\ &= k(\lambda+2\mu)\mathrm{Re}\left\{iA^{(0)}e^{i\eta}-\sum_{m=1}^{\infty} imA_m^{(1)}e^{im\eta}\right\}\\ &= k(\lambda+2\mu)\left\{-A^{(0)}\sin\eta+\sum_{m=1}^{\infty} m\left[R_m^{(1)}\sin m\eta+I_m^{(1)}\cos m\eta\right]\right\},\end{aligned} \tag{A.2}$$

and the displacement discontinuity $\Delta u_y$ at the interface is

$$\begin{aligned}\Delta u_y(\eta) &= \mathrm{Re}\left\{-2\sum_{m=1}^{\infty} A_m^{(1)}e^{im\eta}+A_0^{(3)}-A_0^{(1)}\right\}\\ &= -2\sum_{m=1}^{\infty}\left[R_m^{(1)}\cos m\eta-I_m^{(1)}\sin m\eta\right]+R_0^{(3)}-R_0^{(1)},\end{aligned} \tag{A.3}$$

with $A_m^{(n)}=R_m^{(n)}+iI_m^{(n)}$.

Assume that there is a tension domain $(\alpha_1,\alpha_2)$ within one representative of period $\eta$ (e.g. $-\pi<\eta\le\pi$). Then the boundary condition of Eq. (3) can be rewritten as

$$\begin{cases}\sigma_y(\eta)=K^+\Delta u_y(\eta), & \eta\in(\alpha_1,\alpha_2)\\ \sigma_y(\eta)=K^-\Delta u_y(\eta), & \eta\notin(\alpha_1,\alpha_2)\end{cases} \tag{A.4}$$

Substituting Eqs. (A.2) and (A.3) into Eq. (A.4), we have

$$\sum_{m=1}^{\infty}\left\{\left[mbI_m^{(1)}+2K^+R_m^{(1)}\right]\cos m\eta+\left[mbR_m^{(1)}-2K^+I_m^{(1)}\right]\sin m\eta\right\}$$
$$-bA^{(0)}\sin\eta-K^+\left[R_0^{(3)}-R_0^{(1)}\right]=0,\eta\in(\alpha_1,\alpha_2), \tag{A.5}$$

$$\sum_{m=1}^{\infty}\left\{\left[mbI_m^{(1)}+2K^-R_m^{(1)}\right]\cos m\eta+\left[mbR_m^{(1)}-2K^-I_m^{(1)}\right]\sin m\eta\right\}$$
$$-bA^{(0)}\sin\eta-K^-\left[R_0^{(3)}-R_0^{(1)}\right]=0,\ \eta\notin(\alpha_1,\alpha_2), \tag{A.6}$$

where $b=k(\lambda+2\mu)$.

Define a function $\phi(\eta)$, which is equal to the left portion of Eq. (A.6) when $\eta\notin(\alpha_1,\alpha_2)$, and is zero when $\eta\in(\alpha_1,\alpha_2)$. We thus have

$$K^-\left[R_0^{(3)}-R_0^{(1)}\right]=-\frac{1}{2\pi}\int_{\alpha_1}^{\alpha_2}\varphi(\zeta)d\zeta, \tag{A.7}$$

$$mbI_m^{(1)}+2K^-R_m^{(1)}=\frac{1}{\pi}\int_{\alpha_1}^{\alpha_2}\varphi(\zeta)\cos m\zeta d\zeta,\quad m\ge1, \tag{A.8}$$

$$mbR_m^{(1)}-2K^-I_m^{(1)}=\frac{1}{\pi}\int_{\alpha_1}^{\alpha_2}\varphi(\zeta)\sin m\zeta d\zeta,\quad m\ge1 \tag{A.9}$$

From Eqs. (A.8) and (A.9), we can get the solutions of $R_m^{(1)}$ and $I_m^{(1)}$ as

$$R_m^{(1)} = -\frac{1}{\pi\Delta_m}\left\{2K^- \int_{\alpha_1}^{\alpha_2} \varphi(\zeta)\cos\ m\zeta d\zeta + mb\int_{\alpha_1}^{\alpha_2} \varphi(\zeta)\sin\ m\zeta d\zeta\right\}, \tag{A.10}$$

$$I_m^{(1)} = \frac{1}{\pi\Delta_m}\left\{2K^- \int_{\alpha_1}^{\alpha_2} \varphi(\zeta)\sin\ m\zeta d\zeta - mb\int_{\alpha_1}^{\alpha_2} \varphi(\zeta)\cos\ m\zeta d\zeta\right\}, \tag{A.11}$$

where $\Delta_m = -(2K^-)^2 - m^2b^2$. Substituting these solutions and Eq. (A.7) into Eq. (A.5), we obtain a Fredholm equation of the second kind,

$$\varphi(\eta) + \int_{\alpha_1}^{\alpha_2} \varphi(\zeta)L(\zeta,\eta)d\zeta = bA^{(0)}\ \sin\ \eta,\ \eta\in(\alpha_1,\alpha_2) \tag{A.12}$$

where

$$\begin{aligned} L(\varsigma,\eta) = {} & \frac{4K^-\left(K^+-K^-\right)}{\pi}\sum_{m=1}^{\infty}\frac{\cos\ m(\zeta-\eta)}{m^2b^2+(2K^-)^2} \\ & -\frac{2\left(K^+-K^-\right)}{\pi}\sum_{m=1}^{\infty}\frac{(2K^-)^2}{m^3b^3+mb(2K^-)^2}\sin\ m(\zeta-\eta) \\ & +\frac{2\left(K^+-K^-\right)}{\pi b}[\pi\mathrm{sgn}(\zeta-\eta)-(\zeta-\eta)]+\frac{1}{2\pi}\left(\frac{K^+}{K^-}-1\right). \end{aligned} \tag{A.13}$$

It is noted that both $\phi(\eta)$ and $(\alpha_1,\alpha_2)$ are unknown in Eq. (A.12). The following iterative method is suggested to find $\phi(\eta)$ and $(\alpha_1,\alpha_2)$ by considering the nonlinear boundary condition of Eq. (3):

(i) The iteration starts from $K^-/K^+=1$ (with the same tension and compression stiffness of the interface). In this case, we have linear problem (without higher harmonics) and get the tension zone $(\alpha_1,\alpha_2)$ within a typical period of $\eta$ by considering $\sigma_y(\eta)\geq 0$.
(ii) Applying a small increase to $K^-/K^+$, we obtain $\varphi(\eta)$ by solving Eq. (A.12) numerically with the above estimated value of $(\alpha_1,\alpha_2)$.
(iii) Calculate $\sigma_y(\eta)$ and $\Delta u(\eta)$ through Eqs. (A.2) and (A.3), respectively.
(iv) Determine whether $\Delta u(\alpha_1)=\Delta u(\alpha_2)=0$ and $\Delta u_y(x)\times\sigma_y(x)>0$ are satisfied. If not, we find a new value of $(\alpha_1,\alpha_2)$ according to $\Delta u(\alpha_1)=\Delta u(\alpha_2)=0$ and $\Delta u_y(x)>0$, and then get the solution for $\varphi(\eta)$ from Eq. (A.12).
(v) Repeat step (iii) until $\Delta u(\alpha_1)=\Delta u(\alpha_2)=0$ and $\Delta u_y(x)\times\sigma_y(x)>0$ are satisfied. Then we get final solution of $\varphi(\eta)$ and $(\alpha_1,\alpha_2)$.

Once $\varphi(\eta)$ and $(\alpha_1,\alpha_2)$ are obtained, $R_m^{(3)}$ and $I_m^{(3)}$ can be calculated from Eq. (A.2). Then $A_m^{(3)}$ is calculated by

$$A_m^{(3)} = R_m^{(3)} + iI_m^{(3)} \tag{A.14}$$

## References


[1] Maeva E, Severina I, Bondarenko S, Chapman G, O'Neill B, Severin F, et al. Acoustical methods for the investigation of adhesively bonded structures: a review. Can J Phys 2004;82(12):981–1025.
[2] Yu S, Tong MN, Critchlow G. Use of carbon nanotubes reinforced epoxy as adhesives to join aluminum plates. Mater Des 2010;31:S126–9.
[3] Rokhlin SI, Xie B, Baltazar A. Quantitative ultrasonic characterization of environmental degradation of adhesive bonds. J Adhes Sci Technol 2004;18(3):327–59.
[4] Puthillath P, Rose JL. Ultrasonic guided wave inspection of a titanium repair patch bonded to an aluminum aircraft skin. Int J Adhes Adhes 2010;30(7):566–73.
[5] Ren B, Lissenden CJ. Ultrasonic guided wave inspection of adhesive bonds between composite laminates. Int J Adhes Adhes 2013;45:59–68.
[6] Rothenfusser M, Mayr M, Baumann J. Acoustic nonlinearities in adhesive joints. Ultrasonics 2000;38(1):322–6.
[7] Nagy PB. Fatigue damage assessment by nonlinear ultrasonic materials characterization. Ultrasonics 1998;36(1-5):375–81.
[8] Pruell C, Kim JY, Qu J, Jacobs LJ. Evaluation of fatigue damage using nonlinear guided waves. Smart Mater Struct 2009;18(3):035003.
[9] Shui G, Wang Y, Gong F. Evaluation of plastic damage for metallic materials under tensile load using nonlinear longitudinal waves. NDT E Int 2013;55:1–8.
[10] Achenbach JD, Parikh OK. Ultrasonic analysis of nonlinear response and strength of adhesive bonds. J Adhes Sci Technol 1991;8(5):601–18.
[11] Pangraz S, Arnold W. Quantitative determination of nonlinear binding forces by ultrasonic technique. Rev Prog Quant Nondestr Eval 1994;13:1995–2001.
[12] Tang Z, Cheng A, Achenbach JD. Ultrasonic evaluation of adhesive bond degradation by detection of the onset of nonlinear behavior. J Adhes Sci Technol 1999;13(7):837–54.
[13] Hirsekorn M, Gliozzi A, Nobili M, Abeele K. A 2-D spring model for the simulation of nonlinear hysteretic elasticity. Univ Nonclassical Nonlinearity 2006:287–307.
[14] Delsanto PP, Gliozzi AS, Hirsekorn M, Nobili M. A 2D spring model for the simulation of ultrasonic wave propagation in nonlinear hysteretic media. Ultrasonics 2006;44(3):279–86.
[15] Vanaverbeke S, Van Den Abeele K. Two-dimensional modeling of wave propagation in materials with hysteretic nonlinearity. J Acoust Soc Am 2007;122:58.
[16] An Z, Wang X, Mao J, Li M, Deng M. Theoretical and experimental research on nonlinear spring models of a bonding interface. Chin J Acoust 2012;31(2):113–21.
[17] Nagy PB, Adler L. Nondestructive evaluation of adhesive joints by guided waves. J Appl Phys 1989;66(10):4658–63.
[18] Rokhlin SI, Wang YJ. Analysis of boundary conditions for elastic wave interaction with an interface between two solids. J Acoust Soc Am 1991;89(2):503–15.
[19] Rose JL, Zhu W, Zaidi M. Ultrasonic NDT of titanium diffusion bonding with guided waves. Mater Eval 1998;56(4):535–9.
[20] Lowe M, Cawley P. The applicability of plate wave techniques for the inspection of adhesive and diffusion bonded joints. J Nondestr Eval 1994;13(4):185–200.
[21] Heller K, Jacobs LJ, Qu J. Characterization of adhesive bond properties using Lamb waves. NDT E Int 2000;33(8):555–63.
[22] Seifried R, Jacobs LJ, Qu J. Propagation of guided waves in adhesive bonded components. NDT E Int 2002;35(5):317–28.
[23] Kim J, Jacobs LJ, Qu J, Littles JW. Experimental characterization of fatigue damage in a nickel-base superalloy using nonlinear ultrasonic waves. J Acoust Soc Am 2006;120(3):1266–73.
[24] Shui G, Kim J, Qu J, Wang Y, Jacobs LJ. A new technique for measuring the acoustic nonlinearity of materials using Rayleigh waves. NDT E Int 2008;41(5):326–9.
[25] Website: http://www.netcomposites.com/ikb.
[26] Yan D, Drinkwater BW, Neild SA. Measurement of the ultrasonic nonlinearity of kissing bonds in adhesive joints. NDT E Int 2009;42(5):459–66.
[27] Fatemi A, Yang L. Cumulative fatigue damage and life prediction theories: a survey of the state of the art for homogeneous materials. Int J Fatigue 1998;20(1):9–34.
[28] Cui W. A state-of-the-art review on fatigue life prediction methods for metal structures. J Mar Sci Technol 2002;7(1):43–56.
[29] Xu J, Guo F. Mechanism of fatigue damage evolution and the evolution law. J Mech Eng 2010;46(2):40–6.